



# Stage-dependent differential gene expression profiles of cranial neural crest-like cells derived from mouse-induced pluripotent stem cells

Ayano Odashima<sup>1</sup> · Shoko Onodera<sup>2</sup> · Akiko Saito<sup>2</sup> · Yuuki Ogihara<sup>3</sup> · Tatsuya Ichinohe<sup>3</sup> · Toshifumi Azuma<sup>4</sup>

Received: 6 February 2019 / Accepted: 26 June 2019 / Published online: 11 July 2019  
© The Author(s) 2019

## Abstract

Cranial neural crest cells are multipotent cells that migrate into the pharyngeal arches of the vertebrate embryo and differentiate into various craniofacial organ derivatives. Therefore, migrating cranial neural crest cells are considered one of the most attractive candidate cell sources in regenerative medicine. We generated cranial neural crest like cell (cNCCs) using mouse-induced pluripotent stem cells cultured in neural crest-inducing medium for 14 days. Subsequently, we conducted RNA sequencing experiments to analyze gene expression profiles of cNCCs at different time points after induction. cNCCs expressed several neural crest specifier genes; however, some previously reported specifier genes such as paired box 3 and Forkhead box D3, which are essential for embryonic neural crest development, were not expressed. Moreover, ETS proto-oncogene 1, transcription factor and sex-determining region Y-box 10 were only expressed after 14 days of induction. Finally, cNCCs expressed multiple protocadherins and a disintegrin and metalloproteinase with thrombospondin motifs enzymes, which may be crucial for their migration.

**Keywords** Cranial neural crest · Migratory neural crest · iPS cells · RNA sequencing · Adamts

## Introduction

Stem cell-based tissue engineering is important in the field of oral science because it facilitates the regeneration of damaged tissues or organs [1, 2]. Various stem cell populations

exhibiting regeneration potential in the craniofacial region have been identified. Of these, cranial neural crest cells (cNCCs) are considered one of the most important candidates owing to their role in craniofacial tissue organization [3]. cNCCs comprise a multipotent population of migratory cells that are unique to the vertebrate embryo and can differentiate into various craniofacial organ derivatives [4, 5]. The neural crest (NC) can form teratoma when transplanted into immunocompromised animals [6]. cNCC development involves three stages [7–10]: the neural plate border stage, the premigratory stage, and the migratory stage. During the migratory stage, cNCCs delaminate from the posterior mid-brain and individual rhombomeres in the hindbrain [11] and migrate into the pharyngeal arches to form skeletal elements of the face and teeth and contribute to formation of the pharyngeal glands (the thymus, thyroid, and parathyroid) [12]. Therefore, cNCCs presumably represent a new treatment strategy for diseases of the craniofacial region [13].

Development from the premigratory to migratory stage proceeds swiftly [14]; thus, it is typically difficult to detect the precise time point of this transition [15]. A recent transcriptome analysis of pure populations of migratory cNCCs cells expressing the sex-determining region Y-box 10

---

**Electronic supplementary material** The online version of this article (<https://doi.org/10.1007/s00795-019-00229-2>) contains supplementary material, which is available to authorized users.

---

✉ Toshifumi Azuma  
tazuma@tdc.ac.jp  
Ayano Odashima  
satouayano@tdc.ac.jp

- <sup>1</sup> Department of Oral Health Science Center, Tokyo Dental College, 2-9-18 Misaki-cho, Chiyoda-ku, Tokyo 101-0051, Japan
- <sup>2</sup> Department of Biochemistry, Tokyo Dental College, Tokyo, Japan
- <sup>3</sup> Department of Dental Anesthesiology, Tokyo Dental College, Tokyo, Japan
- <sup>4</sup> Department of Biochemistry, 2-9-18 Misaki-cho, Chiyoda-ku, Tokyo 101-0051, Japan

(*Sox10*) from chicks [16] has substantially improved our understanding of cNCC characteristics. However, whether these cells are in the migratory stage and how long it takes to promote embryonic stem (ES) cell-derived NCCs from the premigratory to migratory stage remains unclear. In recent years, the use of induced pluripotent stem (iPS) cells as a revolutionary approach to treat various medical conditions has garnered much attention [17, 18], and iPS cells as a cell source have shown several evident advantages over ES cells and primary cultured cNCCs in regenerative medicine [16]. In addition, embryonic NC development depends on several environmental factors that influence the regulation of NC progenitors and timing of differentiation; therefore, it is important to elucidate the regulatory gene networks and expression profiles of mouse iPS (miPS) cell-derived cNCCs. Recent advances in next-generation RNA sequencing (RNA-seq) technologies have facilitated comprehensive analysis of gene expression profiles [19–21]. Therefore, in the present study, we used RNA-seq to investigate the gene expression landscape of cNCCs induced from miPS cells. We treated iPS-derived cells with cNCC induction medium for 14 days and performed RNA-seq experiments. Our results indicated that *c-Myc*; ETS proto-oncogene 1, transcription factor (*Ets1*); *Sox10*; a disintegrin and metalloproteinase domain metalloproteinase with thrombospondin motifs (*Adams2*) 2 and 8; protocadherin alpha (*Pcdha*) 2, 5, -7, -11, and -12; protocadherin alpha subfamily C,1 (*Pcdhac1*); and protocadherin gamma subfamily C,3 (*Pcdhgc3*) may be appropriate markers for migratory cNCCs induced from miPS cells.

## Materials and methods

### miPS cell culture

The miPS cells used in the present study (APS0001; iPS-MEF-Ng-20D-17 mouse-induced pluripotent stem cell

line) were purchased from RIKEN BRC (Ibaraki, Japan) [22]. The cells were incubated with inactivated murine embryonic fibroblast (MEF) feeder cells in Dulbecco’s Modified Eagle’s Medium (DMEM; Invitrogen, Carlsbad, CA, USA) supplemented with 15% KnockOut™ Serum Replacement (Invitrogen), 1% nonessential amino acids (Chemicon, Temecula, CA, USA), 1% L-glutamine (Chemicon), 1000 U/mL penicillin–streptomycin (P/S; Invitrogen), and 0.11 mM 2-mercaptoethanol (Wako Pure Chemical Industries Ltd., Osaka, Japan); 60-mm cell culture plates were used for passaging the cells at a density of  $1 \times 10^5$  cells/plate. Cells were grown in 5% CO<sub>2</sub> at 95% humidity, and the culture medium was changed each day.

### Embryoid body (EB) formation and cNCC differentiation

We obtained cultured cNCC cells as described previously [23] (Fig. 1). miPS cells were dissociated with 0.05% trypsin–ethylenediaminetetraacetic acid (EDTA; Invitrogen) and transferred to low-attachment, 10-mm Petri dishes at a density of  $2 \times 10^6$  cells/plate to generate EBs. The generated EBs were cultured in cNCC induction medium comprising a 1:1 mixture of DMEM and F12 nutrient mixture (Invitrogen) and then in Neurobasal™ medium (Invitrogen) supplemented with  $0.5 \times N2$  (Invitrogen),  $0.5 \times B27$  (Invitrogen), 20 ng/mL basic fibroblast growth factor (Reprocell, Yokohama, Japan), 20 ng/mL epidermal growth factor (Peprotech, Offenbach, Germany), and 1% P/S for 4 days; the medium was changed every other day. After 4 days, day 0 (d0) EBs were collected and transferred to 60-mm cell culture plates coated with 1 µg/mL collagen type I (Advanced BioMatrix, San Diego, CA, USA). The cells were then subcultured in the same medium; the medium changed every other day, and any rosette-forming cells were eliminated. After 7–10 days, d7 cells were dissociated with 0.05% trypsin–EDTA and transferred to 60-mm

**Fig. 1** The experimental protocol used to induce the formation of cranial neural crest cells (cNCCs) from mouse-induced pluripotent stem (miPS) cells. The photographs show miPS cells at four different stages: initial miPS cells, embryoid body (EB) on day 0 (d0), and cNCCs on d7 and d14. Small circles represent miPS cells; large circles represent EBs; ellipses represent d7 and d14 cells. Scale bar 50 µm

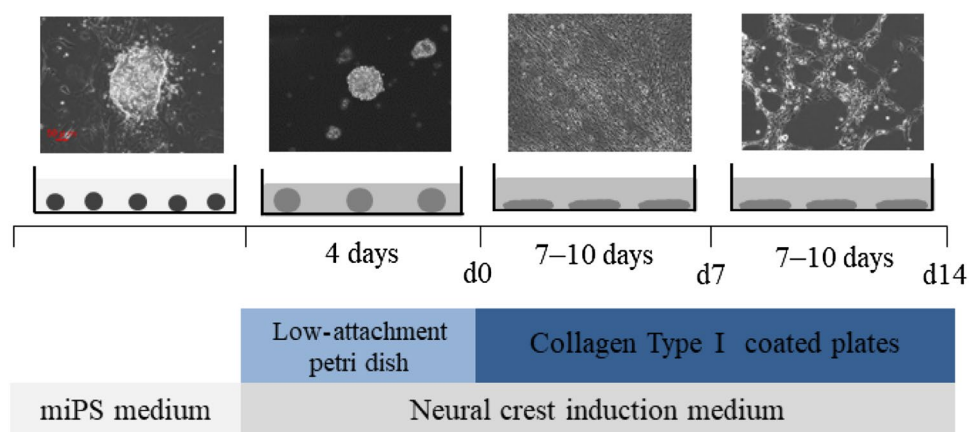


**Table 1** Primers used for quantitative reverse transcription polymerase chain reaction (qRT-PCR)

Gene	Forward primer sequence	Reverse primer sequence
<i>18S rRNA</i>	CGGACAGGATTGACAGATTG	CGCTCCACCAACTAAGAACG
<i>Ngfr (p75NTR)</i>	ACTGAGCGCCAGTTACGC	CGTAGACCTTGTGATCCATCG
<i>Snail (Snail)</i>	CTTGTGTCTGCACGACCTGT	AGGAGAATGGCTTCTCACCA
<i>Snai2 (Slug)</i>	CATTGCCTTGTCTGCAAG	CAGTGAGGGCAAGAGAAAGG
<i>Sox9</i>	GTACCCGCATCTGCACAAC	CTCCTCCACGAAGGGTCTCT
<i>Sox10</i>	ATGTCAGATGGGAACCCAGA	GTCTTTGGGGTGGTTGGAG

cell culture plates coated with 1 µg/mL collagen type I at a density of  $1 \times 10^5$  cells/plate to generate d14 cells. This process was repeated three times. The cells from each of these passages were collected for RNA extraction.

### O9-1 cell culture

O9-1 cells, a mouse cNCC line, were purchased from Millipore (Billerica, MA, USA) and cultured as a control, as previously described [24].

### RNA extraction and quantitative reverse transcription polymerase chain reaction analysis (qRT-PCR)

The expression of representative NC markers, namely nerve growth factor receptor (*Ngfr*), snail family transcriptional repressor (*Snai*) 1 and 2, and *Sox9* and *10*, was analyzed using qRT-PCR analysis. Total RNA was extracted using QIAzol<sup>®</sup> reagent (Qiagen, Valencia, CA, USA) according to the manufacturer's protocol, and RNA purity was assessed using NanoDrop<sup>®</sup> ND-1000 spectrophotometer (Thermo Fisher Scientific, Waltham, MA, USA). Each RNA sample exhibited an A260/A280 ratio of > 1.9. Complementary DNA (cDNA) was synthesized using a high-capacity cDNA reverse transcription kit (Applied Biosystems, Foster City, CA, USA), and qRT-PCR analysis was performed with Premix Ex Taq<sup>™</sup> reagent (Takara Bio Inc., Otsu, Japan) according to the manufacturer's protocol using Applied Biosystems<sup>®</sup> 7500 Fast Real-Time PCR System; the primer sequences are presented in Table 1. All samples were normalized to 18S ribosomal RNA levels. Relative expressions of genes of interest were analyzed using the  $\Delta\Delta C_t$  method and were compared among the groups using analysis of variance, followed by the Bonferroni test when significant differences were detected among the groups. A significance level of  $p < 0.05$  was used for all analyses, and all data were expressed as mean values and standard deviations.

### Immunohistochemistry

The cells were fixed with 4% paraformaldehyde (Wako Pure Chemical Industries Ltd.) for 15 min followed by methanol

(Wako Pure Chemical Industries Ltd) for 5 min. After washing, the nonspecific binding of antibodies was blocked by adding 5% bovine serum albumin (BSA; Wako Pure Chemical Industries Ltd.) in a phosphate-buffered saline with 0.5% Triton X-100 (PBST) for 1 h. The cells were then incubated with the primary antibodies Snai1 1:50 for Rabbit polyclonal anti-Snai1 (26183-1-AP; Proteintech Group, Inc. Chicago, IL, USA.) and Sox10 1:500 for Mouse monoclonal anti-Sox10 (AMAb91297; Atlas Antibodies, Bromma, Sweden.) in PBST for 2 nights at 4 °C. We conducted that the positive control of Snai1 was O9-1 cells (cranial neural crest cells) and the positive control of Sox10 was DP cells (dental pulp cells). The negative control of Snai1 and Sox10 was SNL cells (fetus fibroblast cells) (Fig. S1). They were then incubated in the secondary antibodies fluorescein isothiocyanate Alexa Flour 488-conjugated affinity purified Goat anti-Rabbit IgG (H&L) (ab150077; Abcam, Cambridge, MA, USA) at a dilution of 1:500 for Snai1 and Alexa Flour 568-conjugated affinity purified Goat anti-Mouse IgG (H&L) (A-11004; Invitrogen) at a dilution of 1:500 for Sox10 in PBST for 1 h. Eventually, the cells were stained with 4,6-diamidino-2-phenylindole (DAPI; Sigma, Livonia, MI, USA) to visualize the nuclear DNA.

### RNA-seq

Total RNA from each sample was used to construct libraries with the Illumina TruSeq Stranded mRNA LT Sample Prep Kit (Illumina, San Diego, CA, USA), according to the manufacturer's instructions. Polyadenylated mRNAs are commonly extracted using oligo-dT beads, following which the RNA is often fragmented to generate reads that cover the entire length of the transcripts. The standard Illumina approach relies on randomly primed double-stranded cDNA synthesis, followed by end-repair, dsDNA adapter ligation, and PCR amplification. The multiplexed libraries were sequenced as 125-bp paired-end reads using the Illumina HiSeq 2500 system (Illumina). Prior to performing any analysis, quality of the data was confirmed and read cleaning, such as adapter removal and simple quality filtering, was performed using Trimmomatic (ver. 0.32). Subsequently, the paired-end reads were mapped to the mouse genome reference sequence GRCm38 using the Burrows–Wheeler

Aligner (ver. 0.7.10). The number of sequence reads mapped to each gene domain using SAM tools (ver. 0.1.19) was counted, and the reads per kilobase of transcript per 1 million mapped reads (RPKM) for known transcripts were calculated to normalize the expression level data to gene length and library size, thereby facilitating the comparison of different samples.

## Results

### Gene expression profiles and immunohistochemistry of cNCCs derived from miPS cells

Expressions of the NC markers *Ngfr*, *Snai1*, *Snai2*, *Sox9*, and *Sox10* were examined by qRT-PCR in cNCCs derived from miPS cells as well as in O9-1 cells as a control. Expression of all genes except *Ngfr* and *Sox10* was detected in O9-1 cells [24]. In contrast, expressions of all genes were detected in cNCCs, with the premigratory NC markers *Ngfr*, *Snai1*, and *Snai2* exhibiting the highest expression levels in d7 cells and the migratory and cranial NC markers *Sox9* and *Sox10* exhibiting the highest expression levels in d14 cells (Fig. 2a). The strongest immunofluorescent staining was detected for *Snai1* and *Sox10* in d7 and d14 cells, respectively (Fig. 2b).

### NC specifier transcription factors

We conducted a literature search of NC specifier transcription factors identified in vivo [16, 25–80] (Tables 2, 3) and compared these reports with our RNA-seq results. The relative expressions of genes that underwent a significant change in expression are presented in Fig. 3a.

The transcription factor AP-2 alpha (*Ap2*) along with paired box 3 (*Pax3*) and zinc finger protein of the cerebellum 1 (*Zic1*), both of which are regulated by *Ap2*, were the most highly expressed genes in d7 cells (Fig. 3a). *Pax6*, which has been reported in human ES and iPS-derived NC cells (Tables 2, 3), was detected in both d7 and d14 cells, whereas *Pax7*, which has not previously been reported in the mouse NC, was detected in the d7 cells (Fig. 3a). In contrast, the homeobox genes *gastrulation brain homeobox 2* (*Gbx2*), *msh homeobox 1* (*Msx1*), *distal-less homeobox 3* (*Dlx3*), *Zic2*, and *Zic3* were not detected in d7 or d14 cells, and the homeobox genes *Zic1* and *Dlx5* were only expressed in the d7 cells, despite these having been reported in the NC of a range of species (Table 2); however, *Meis homeobox 2* (*Meis2*) was expressed in both d7 and d14 cells.

The MYCN proto-oncogenes, bHLH transcription factor (*N-myc*) and *c-Myc*, have been reported in NCCs (Table 3); however, *c-Myc* expression was detected in d7 and d14 cells

(Fig. 3a), while *N-myc* was not. Furthermore, there was a gradual and substantial downregulation of the winged-helix transcription factor Forkhead box D3 (*FoxD3*) (Fig. 3a), which is an important factor for maintaining the pluripotency of ES cells and a key NC specifier that has been implicated in multiple stages of NC development and NCC migration in embryos of various species (Tables 2, 4).

The premigratory NC markers *Ngfr*, heart and neural crest derivatives expressed 2 (*Hand2*), *Snai1*, and *Snai2* were only detected in the d7 cells; however, other premigratory NC markers, such as the platelet derived growth factor receptor, alpha polypeptide (*Pdgfra*); 6-phosphofructo-2-kinase/fructose-2,6-biphosphatase 4 (*Pfkfb4*); inhibitor of DNA binding 2 (*Id2*), *Id3*, and *Id4*; and nestin (*Nes*) were detected in both d7 and d14 cells (Fig. 3a).

Expression of migratory NC markers such as *Sox5*, -6, -8, -9, and -10, which encode members of the sex-determining region Y (SRY)-related high mobility group (HMG)-box family of transcription factors and are crucial in several aspects of NCCs, were detected in d7 or d14 cells. *Sox10*, a known marker for migratory cNCCs in various species (Table 2), was only detected in d14 cells similar to the other migratory NC markers. Twist family bHLH transcription factor 1 (*Twist1*), which is activated via various signal transduction pathways and is crucial for E-cadherin downregulation, as well as beta-1,3-glucuronyltransferase 1 (*B3gat1/Hnkl*), which plays a role in the formation of CD57 epitope, was detected in both d7 and d14 cells. In contrast, the expression of the trunk NC markers lit guidance ligand 1/2 (*Slit1/2*), which plays an important role in trunk NC cell migration toward ventral sites, was upregulated only in d7 cells (Fig. 3a).

Finally, expressions of tenascin C (*Tnc*), cadherin-6 (*Cdh6*), and ras homolog family member B (*Rhob*), all of which are related to cell adhesion and motility [81–85], were significantly increased in both d7 and d14 cells (Fig. 3b).

### Metzincin superfamily zinc proteinase and protocadherin superfamily

Members of the metzincin superfamily are proteinases that carry a zinc ion at their active site. This family includes the matrix metalloproteinases (Mmps), Adam, and Adamts, all of which have gained attention as factors involved in cancer cell invasion and migration. *Mmp2*, -11, -14, -15, -16, -24, and -28 were significantly upregulated in cNCCs (Fig. 4a), all of which except *Mmp24* are membrane-bound. *Mmp11* and -28 were only expressed in d7 cells, whereas all other Mmps were detected in both d7 and d14 cells (Fig. 4a, b).

Only *Adam1a*, -8, -10, and -12 were upregulated in both d7 and d14 cells (Fig. 4c, d); this is contrary to reports that the members of this family are important in NC migration and that *Adam-10*, -12, -15, -19, and -33 are expressed in the

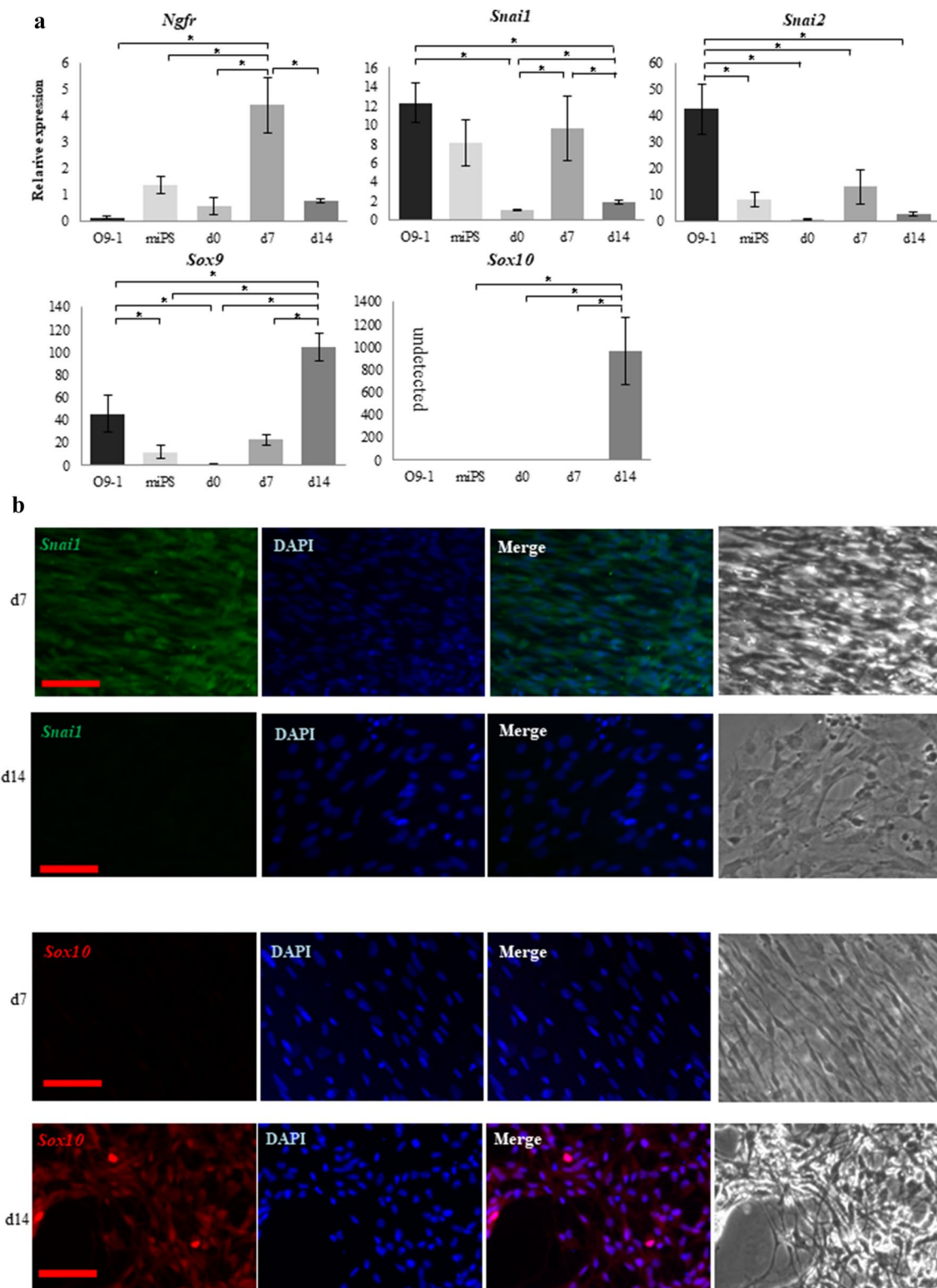


**Fig. 2** Comparison between O9-1 cells and cranial neural crest cells (cNCCs) derived from mouse-induced pluripotent stem (miPS) cells using quantitative reverse transcription polymerase chain reaction (qRT-PCR) and immunostaining. **a** Expression of the premigratory neural crest (NC) markers *Ngfr*, *Snai1*, and *Snai2* and the migratory NC and cNC markers *Sox9* and *Sox10*. Expressions of the premigratory NC markers increased in day 7 (d7) cells, whereas those of the

migratory markers increased in d14 cells. *Sox10* was not detected in O9-1 cells. Each experiment was performed in triplicate, with values representing mean  $\pm$  SD. Groups were compared using ANOVA, followed by the Bonferroni test:  $*p < 0.05$ . **b** Immunostaining of d7 and d14 cells. *Sox10* was more highly expressed in the d14 cells, whereas *Snai1* was more highly expressed in the d7 cells. Scale bar 50  $\mu$ m

**Table 2** Neural crest (NC) genes that have previously been examined in vivo

	Reference	Vertebrates					RNA-seq	
		L	Z	X	C	M	d7	d14
Cranial	25 Antonellis A et al., 2006				○			
	26 Betancur P et al., 2010				○			
	27 Rinon A et al., 2011				○			
	28 Hari L et al., 2012					○	×	○
	16 Simões-Costa M et al., 2014					○		
	29 Murko C et al., 2016					○		
	30 Spokony RF et al., 2002		○				○	○
	28 Hari L et al., 2012					○		
	16 Simões-Costa M et al., 2014				○		○	○
	31 Perez-Alcala S et al., 2004				○		○	○
	28 Hari L et al., 2012					○	○	×
	16 Simões-Costa M et al., 2014				○		○	×
	26 Betancur P et al., 2010				○		×	○
	32 Barembaum M et al., 2013				○			
	33 Nagai T et al., 1997					○	○	×
	33 Nagai T et al., 1997					○	×	×
	34 Teslla JJ et al., 2013		○				×	×
	33 Nagai T et al., 1997					○	×	×
	16 Simões-Costa M et al., 2014					○	×	×
	16 Simões-Costa M et al., 2014					○	×	○
	16 Simões-Costa M et al., 2014					○	×	×
	16 Simões-Costa M et al., 2014					○	×	○
	35 Das A et al., 2012			○				
	16 Simões-Costa M et al., 2014					○	○	○
	16 Simões-Costa M et al., 2014					○	○	×
	16 Simões-Costa M et al., 2014					○	×	×
35 Das A et al., 2012			○			○	○	
36 Machon O et al., 2015					○	○	○	

Gene groups

- Homeobox genes
- SRY-related HMG box genes

Vertebrates

- L *Lamprey*
- Z *Zebrafish*
- X *Xenopus*
- C *Chick*
- M *Mouse*

Open circles indicate genes that were upregulated on day 7 (d7) or d14 compared with d0 [log fold change (FC) > 1,  $p < 0.01$ , false discovery rate (FDR) < 0.05], whereas crosses indicate genes that were not upregulated

mouse NC [86]. Moreover, various *Adamts* family genes, which are important for connective tissue organization and cell migration, were upregulated in either d7 or d14 cells (Fig. 4c, d). In particular, *Adamts1* expression was markedly increased, whereas *Adamts2* and *-8* expressions, which are presumably important in cancer cell invasion [87–89], increased in the later stages of differentiation.

Most *Pcdh* genes, which are involved in cell adhesion [90], were upregulated in d7 and d14 cells (Table 5); however, *Pcdha2*, *-5*, *-7*, *-11*, and *-12*; *Pcdhac1*; and *Pcdhgc5* were only upregulated in d14 cells.

## Discussion

In the present study, we derived cells from miPS which are closely migratory cNCCs genes. Previously, NCCs have been derived from ES or iPS cells using various approaches [91–110], and the protocol used in the present study was based on the methods outlined by Bajpai et al. [23]; however, few studies have investigated changes in the properties of cNCCs at different time points after induction.

In the present study, d7 and d14 cells expressed typical NC markers, such as *Ngfr*, *Snai1*, and *Snai2*. In contrast, O9-1 cells (controls) did not express *Ngfr*, suggesting that cNCCs derived from miPS cells are better than O9-1 cells

for evaluating cNCC characteristics [24]. Moreover, unlike O9-1 cells, d14 cells expressed markedly high levels of *Sox10*, which is considered a reliable marker for migratory cNCCs. Since cNCCs are involved in craniofacial tissue organization, several reports are available on their gene expression profiles; however, these reports show varying results with species and protocols. Moreover, cNCCs rapidly differentiate in the embryo [14]; thus, it is considerably difficult to synchronize the timing of isolation to a particular point during their development. Furthermore, migratory cNCCs intermingle with other cell types in the embryo, further complicating the isolation and characterization of a pure cell population. Consequently, there have been few reports on cNCC markers [16, 25–36]. Simões-Costa et al. [16] successfully isolated *Sox10*-positive cNCCs from chicken embryos and analyzed their gene profiles. Similarly, we detected *Sox10* expression in d14 cNCCs. Reportedly, there are multiple NCC populations [11], and iPS cells can differentiate into numerous different NCC populations in the same culture. Therefore, this diversity in populations may explain the discrepancies in results; however, under the conditions used in the present study, *c-Myc*; *Ets1*; *Sox10*; *Adamts2*; *Adamts8*; *Pcdha2*, *-5*, *-7*, *-11*, and *-12*; *Pcdhac1*, and *Pcdhgc3* may represent useful markers for migratory cNCCs. Furthermore, our results indicated that d7 cells were in the premigratory



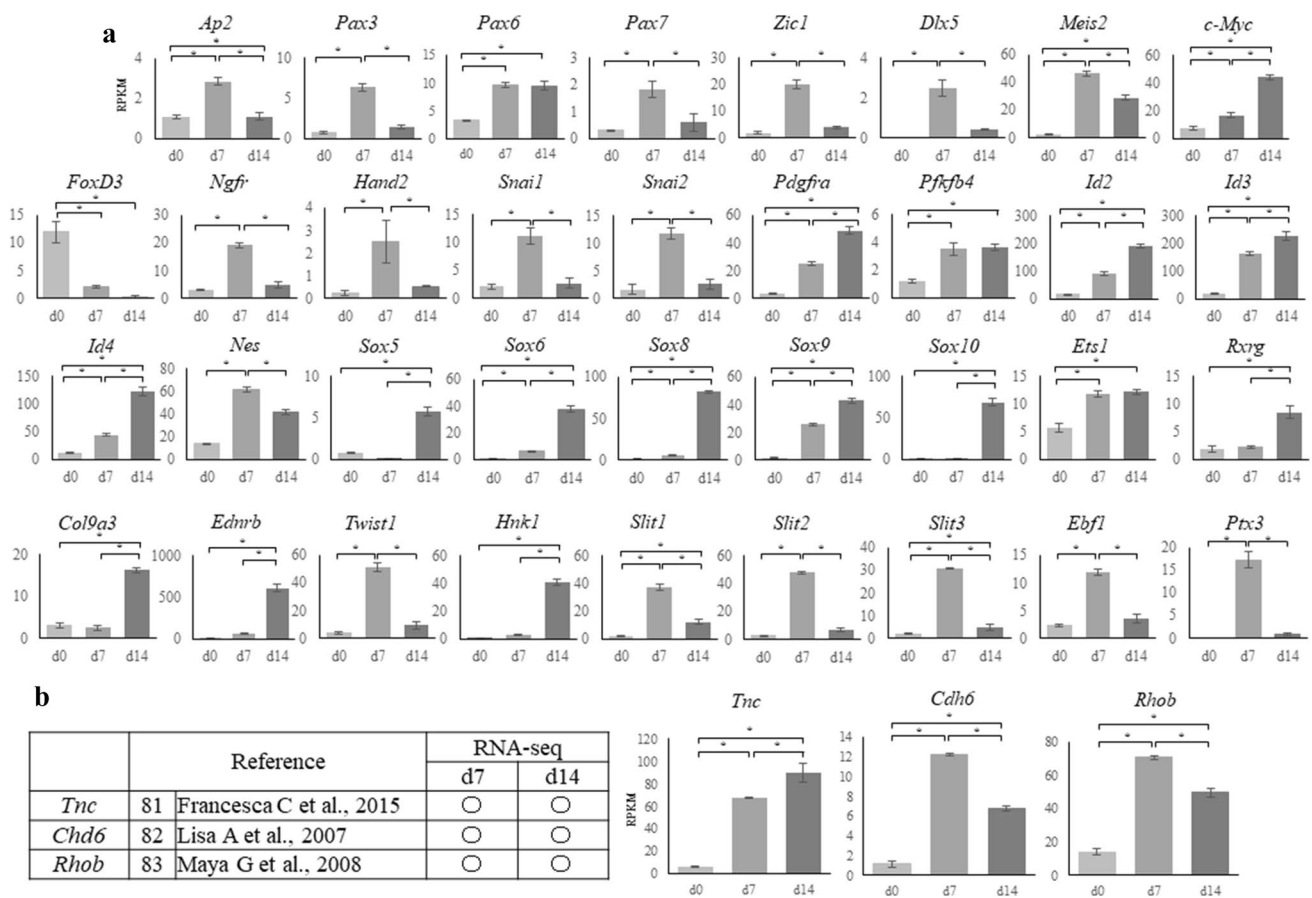


**Fig. 3** RNA sequencing results for cranial neural crest cells (cNCCs) differentiated from mouse-induced pluripotent stem (miPS) cells. **a** Expression of each of the genes listed in Table 2 at day 0 (d0), d7, and d14 after induction. Sex-determining region Y (SRY)-related high mobility group (HMG) box genes showed the highest upregulation in d14 cells. The vertical axis reveals reads per kilobase of exon per million mapped reads (RPKM), and the horizontal axis indicates time. Each experiment was performed in triplicate, with values representing mean  $\pm$ SD. Groups were compared using ANOVA, followed by the Bonferroni test: \* $p < 0.05$ . **b** Expression of genes that have not

been examined during the neural crest stages in vivo. *Tnc* showed the highest upregulation in d14 cells, whereas *Cha6* and *Rhob* were upregulated in day 7 (d7) cells. The vertical axis indicates reads per kilobase of exon per million mapped reads (RPKM), and the horizontal axis indicates time. Open circles indicate genes upregulated in d7 or d14 compared with d0 [log fold change (FC) > 1,  $p < 0.01$ , false discovery rate (FDR) < 0.05]. Each experiment was performed in triplicate, with values representing mean  $\pm$ SD. Groups were compared using ANOVA, followed by the Bonferroni test: \* $p < 0.05$

stage despite expressing numerous NC markers. Therefore, cNCCs derived from miPS cells required > 14 days to become migratory in vitro, and this duration is considerably longer than that observed in the mouse embryos in vivo under the same conditions [111].

The use of RNA-seq facilitates the normalization of expression levels of different genes, allowing comparisons between samples. In our triplicate experiments, none of the induced cNCCs expressed several homeobox genes considered to be expressed in the early stages of cNCC differentiation. In particular, we did not observe *FoxD3* expression in either d7 or d14 cells, although it has been recognized as one of the key transcription factors in cNCCs [112]. These contradictory results suggest that cNCCs derived from miPS

cells express distinct gene regulatory networks. *FoxD3*, a pluripotent stem cell marker gene that plays an important role in maintaining pluripotency, is expressed at different time points in different cells, but its expression decreases in a time-dependent manner [41], indicating that *FoxD3* may not be a key regulator in iPS-derived cNCCs. However, we speculate that iPS cells express sufficient levels of *FoxD3* to differentiate into cNCCs.

Protocadherins belong to the cadherin superfamily and are involved in intercellular interactions [90], whereas metzincins are key proteinases that facilitate cell migration [42]. Unfortunately, the abundances of members of these families hindered their analysis; however, because RNA-seq enabled us to comprehensively evaluate the gene expression profiles,





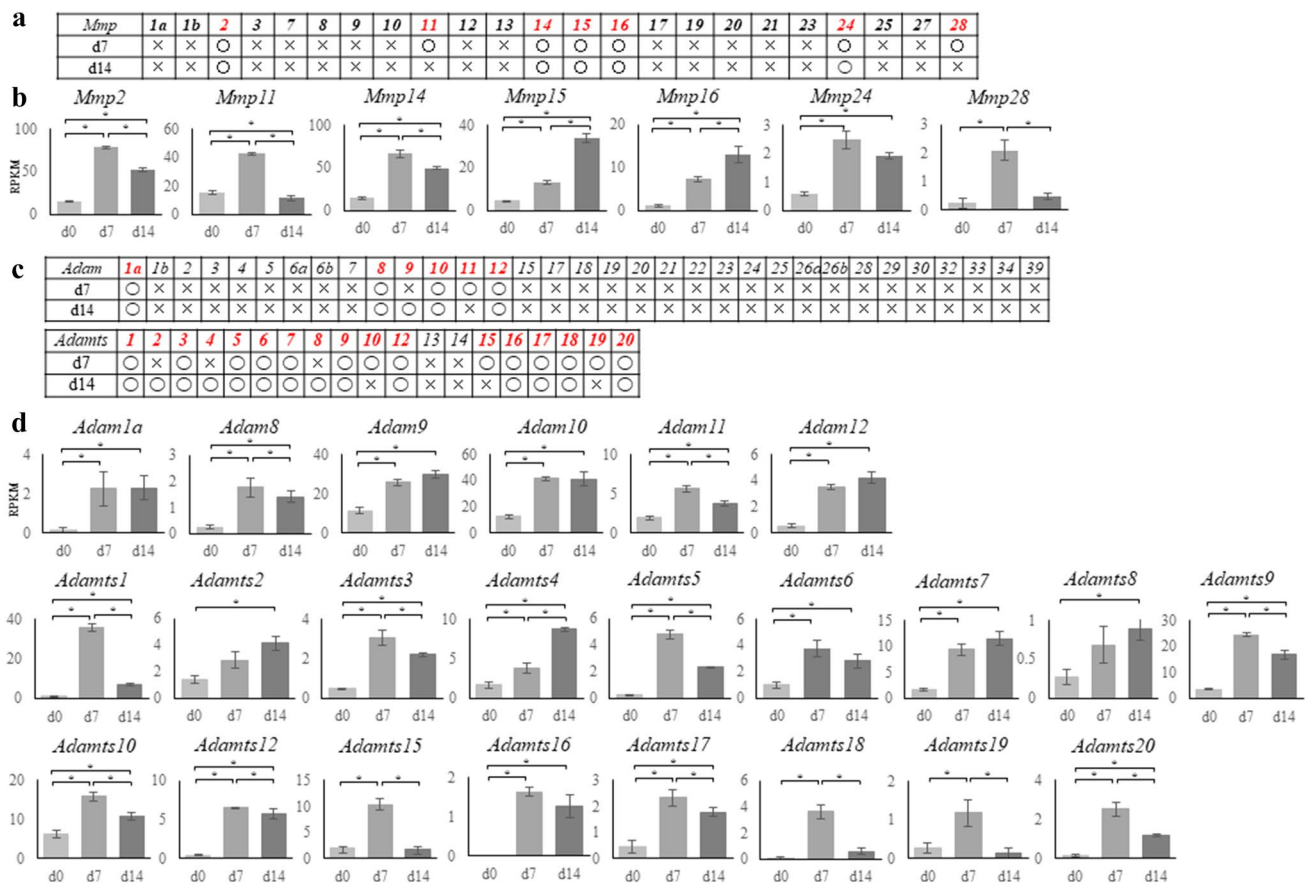


**Fig. 4** RNA sequencing results for the matrix metalloproteinase (*Mmp*), a disintegrin and metalloproteinase (*Adam*), and a disintegrin and metalloproteinase with thrombospondin motifs (*Adamts*) gene families. **a** Expressions of *Mmp* family genes in mouse. Round marks alongside day 7 (d7) or d14 cells indicate that the genes were upregulated compared with d0 [log fold change (logFC) > 1,  $p < 0.01$ , false discovery rate (FDR) < 0.05], whereas cross marks indicate lack of upregulation. **b** Graphical representation of the upregulation of *Mmp2*, *-11*, *-14*, *-15*, *-16*, *-24*, and *-28* in d7 or d14 cells. *Mmp15* and *-16* showed the highest upregulation in d14 cells. The vertical axis indicates reads per kilobase of exon per million mapped reads (RPKM), and the horizontal axis indicates time. Each experiment was performed in triplicate, with values representing mean  $\pm$  SD. Groups

were compared using ANOVA, followed by the Bonferroni test:  $*p < 0.05$ . **c** Expressions of *Adam* and *Adamts* genes in mouse. Round marks alongside d7 or d14 cells indicate that the genes were upregulated compared with d0 (logFC > 1,  $p < 0.01$ , FDR < 0.05), whereas cross marks indicate lack of upregulation. **d** Graphical representation of the upregulation of *Adam1a* and 8–12, and *Adamts1*–10, -12, and 15–20 in the d7 or d14 cells. *Adam2*, -4, -7, and -8, and *Adamts9* and -12 showed the highest upregulation in d14 cells. The vertical axis indicates reads per kilobase of exon per million mapped reads (RPKM), and the horizontal axis indicates time. Each experiment was performed in triplicate, with values representing mean  $\pm$  SD. Groups were compared using ANOVA, followed by the Bonferroni test:  $*p < 0.05$

we were able to focus on expressions of all procadherin and metazincin family members. As expected, we observed that several *Adam* and *Adamts* genes were upregulated, with most of the *Admats* genes showing significantly increased expression. The *Adam* genes with increased expression in cNCCs were membrane-bound, whereas *Adamts* genes which secreted proteinases, indicating that the expression of various *Adamts* may allow the matrix to be digested more efficiently and that each proteinase may be capable of digesting a different type of extracellular matrix protein [42]. Therefore, the secretion of various *Adamts* and *Pcdh* proteins may play a crucial role in cNCC migration.

## Conclusion

In summary, cNCCs derived from miPS exhibited RNA expression profiles that partly overlap with previously reported profiles. These cells may be useful for the regeneration of tissue formed by NCCs (osteoblast, melanocyte, and glial cells). We observed that although the resulting cNCCs exhibited several NC specifiers, they lacked some of the specifiers, indicating that a distinct molecular network may regulate gene expression in miPS-derived cNCCs. Moreover, our results indicated that *c-Myc*; *Ets1*; *Sox10*; *Adamts2* and -8; *Pcdha2*, -5, -7, -11, and -12; *Pcdhac1*; and *Pcdhgc3* may represent appropriate markers for migratory miPS-derived

**Table 5** Expression of the protocadherin superfamily based on RNA sequencing data

<i>Pcdh</i>	1	7	8	9	10	11	12	15	17	18	19	20
d7	×	○	○	○	○	○	×	×	○	○	○	×
d14	×	○	○	○	○	○	×	○	○	○	○	×

<i>Pcdha</i>	1	2	3	4	5	6	7	8	9	10	11	12
d7	○	×	○	○	×	○	×	○	○	○	×	×
d14	○	○	○	○	○	○	○	○	○	○	○	○

<i>Pcdhb</i>	1	2	3	4	5	6	7	8	9	10	11	12	13	14	15	16	17	18	19	20	21	22
d7	×	○	○	○	○	○	○	○	○	○	○	○	○	○	○	○	○	○	○	○	○	○
d14	×	○	○	○	○	○	○	○	○	○	○	○	○	○	○	○	○	○	○	○	○	○

<i>Pcdhac</i>	1	2
d7	×	○
d14	○	○

<i>Pcdhgc</i>	3	4	5
d7	○	○	×
d14	○	○	○

<i>Pcdhgb</i>	1	2	4	5	6	7	8
d7	○	○	○	○	○	○	○
d14	○	○	○	○	○	○	○

Open circles indicate genes that were upregulated on day 7 (d7) or d14 compared with d0 [ $\log$  fold change (FC)  $> 1$ ,  $p < 0.01$ , false discovery rate (FDR)  $< 0.05$ ], whereas crosses indicate genes that were not upregulated

cNCCs. Finally, cNCCs expressed a wide spectrum of genes encoding Adamts family enzymes that may be crucial for their migration.

**Acknowledgements** We are grateful to Professor T. Azuma, MD, PhD, Department of Biochemistry, and Professor T. Ichinohe, DDS, PhD, Department of Dental Anesthesiology, for their guidance. We also thank S. Onodera and A. Saito, Department of Biochemistry.

**Funding** The funding was received by Ministry of Science and Technology (Grant nos. KIBANKENNKYU(B)18H03007 and 18K09753 KIBANKENNKYU(C)).

### Compliance with ethical standards

**Conflict of interest** The authors declare that they have no conflicts of interest.

**Open Access** This article is distributed under the terms of the Creative Commons Attribution 4.0 International License (<http://creativecommons.org/licenses/by/4.0/>), which permits unrestricted use, distribution, and reproduction in any medium, provided you give appropriate

credit to the original author(s) and the source, provide a link to the Creative Commons license, and indicate if changes were made.

### References

- Luan X, Dangaria S, Ito Y, Walker GG, Jin T, Schmidt MK, Galang MT, Druzinsky R (2009) Neural crest lineage segregation: a blueprint for periodontal regeneration. *J Dent Res* 88(9):781–791
- Malhotra N (2016) Induced pluripotent stem (iPS) cells in dentistry: a review. *Int J Stem Cells* 9(2):176–185
- Knight RD, Schilling TF (2006) Cranial neural crest and development of the head skeleton. *Adv Exp Med Biol* 589:120–133
- Theveneau E, Mayor R (2011) Collective cell migration of the cephalic neural crest: the art of integrating information. *Genesis* 49(4):164–176
- Chai Y, Jiang X, Ito Y, Bringas P Jr, Han J, Rowitch DH, Soriano P, McMahon AP, Sucov HM (2000) Fate of the mammalian cranial neural crest during tooth and mandibular morphogenesis. *Development* 127(8):1671–1679
- McConnell AM, Mito JK, Ablain J, Dang M, Formichella L, Fisher DE, Zon LI (2018) Neural crest state activation in NRAS

- driven melanoma, but not in NRAS-driven melanocyte expansion. *Dev Biol* 449(17):30855–30862
7. Meulemans D, Bronner-Fraser M (2004) Gene-regulatory interactions in neural crest evolution and development. *Dev Cell* 7(3):291–299
  8. Steventon B, Carmona-Fontaine C, Mayor R (2005) Genetic network during neural crest induction: from cell specification to cell survival. *Semin Cell Dev Biol* 16(6):647–654
  9. Simões-Costa M, Bronner ME (2015) Establishing neural crest identity: a gene regulatory recipe. *Development* 142(2):242–257
  10. Martik ML, Bronner ME (2017) Regulatory logic underlying diversification of the neural crest. *Trends Genet* 33(10):715–727
  11. Minoux M, Rijli FM (2010) Molecular mechanisms of cranial neural crest cell migration and patterning in craniofacial development. *Development* 137(16):2605–2621
  12. Mayor R, Theveneau E (2013) The neural crest. *Development* 140(1):2247–2251
  13. Okuno H, Mihara FR, Ohta S, Fukuda K, Kurosawa K, Akamatsu W, Sanosaka TS, Kohyama J, Hayashi K, Nakajima K, Takahashi T, Wysocka J, Kosaki K, Okano H (2017) CHARGE syndrome modeling using patient-iPSCs reveals defective migration of neural crest cells harboring CHD7 mutations. *eLife* 6:e21114
  14. Simoes-Costa M, Bronner ME (2016) Reprogramming of avian neural crest axial identity and cell fate. *Science* 352(6293):1570–1573
  15. Milet C, Monsoro-Burq AH (2012) Neural crest induction at the neural plate border in vertebrates. *Dev Biol* 366(1):22–33
  16. Simões-Costa M, Tan-Cabugao J, Antoshechkin I, Sauka-Spengler T, Bronner ME (2014) Transcriptome analysis reveals novel players in the cranial neural crest gene regulatory network. *Genome Res* 24(2):281–290
  17. Doi D, Samata B, Katsukawa M, Kikuchi T, Morizane A, Ono Y, Sekiguchi K, Nakagawa M, Parmar M, Takahashi J (2014) Isolation of human induced pluripotent stem cell derived dopaminergic progenitors by cell sorting for successful transplantation. *Stem Cell Rep* 2(3):337–350
  18. Nakane T, Masumoto H, Tinney JP, Yuan F, Kowalski WJ, Ye F, LeBlanc AJ, Sakata R, Yamashita JK, Keller BB (2017) Impact of cell composition and geometry on human induced pluripotent stem cells-derived engineered cardiac tissue. *Sci Rep* 7:45641
  19. Gallego RI, Pai AA, Tung J, Gilad Y (2014) RNA-seq: impact of RNA degradation on transcript quantification. *BMC Biol* 12:42
  20. Wang Z, Gerstein M, Snyder M (2009) RNA-Seq: a revolutionary tool for transcriptomics. *Nat Rev Genet* 10(1):57–63
  21. Mortazavi A, Williams BA, McCue K, Schaeffer L, Wold B (2008) Mapping and quantifying mammalian transcriptomes by RNA-Seq. *Nat Methods* 5(7):621–628
  22. Okita K, Ichisaka T, Yamanaka S (2007) Generation of germline competent induced pluripotent stem cells. *Nature* 448(7151):313–317
  23. Bajpai R, Chen DA, Rada-Iglesias A, Zhang J, Xiong Y, Helms J, Chang CP, Zhao Y, Swigut T, Wysocka J (2010) CHD7 cooperates with PBAF to control multipotent neural crest formation. *Nature* 463(7283):958–962
  24. Ishii M, Arias AC, Liu L, Chen YB, Bronner ME, Maxson RE (2012) A stable cranial neural crest cell line from mouse. *Stem Cells Dev* 21(17):3069–3080
  25. Antonellis A, Bennett WR, Menhenniott TR, Prasad AB, Lee-Lin SQ, NISC Comparative Sequencing Program, Green ED, Paisley D, Kelsh RN, Pavan WJ, Ward A (2006) Deletion of long-range sequences at Sox10 compromises developmental expression in a mouse model of Waardenburg-Shah (WS4) syndrome. *Hum Mol Genet* 15(2):259–271
  26. Betancur P, Bronner-Fraser M, Sauka-Spengler T (2010) Genomic code for Sox10 activation reveals a key regulatory enhancer for cranial neural crest. *Proc Natl Acad Sci USA* 107(8):3570–3575
  27. Rinon A, Molchadsky A, Nathan E, Yovel G, Rotter V, Sarig R, Tzahor E (2011) p53 coordinates cranial neural crest cell growth and epithelial–mesenchymal transition/delamination processes. *Development* 138(9):1827–1838
  28. Hari L, Miescher I, Shakhova O, Suter U, Chin L, Taketo M, Richardson WD, Kessaris N, Sommer L (2012) Temporal control of neural crest lineage generation by Wnt/ $\beta$ -catenin signaling. *Development* 139(12):2107–2117
  29. Murko C, Bronner ME (2016) Tissue specific regulation of the chick Sox10E1 enhancer by different Sox family members. *Dev Biol* 422(1):47–57
  30. Spokony RF, Aoki Y, Saint-Germain N, Magner-Fink E, Saint-Jeannet JP (2002) The transcription factor Sox9 is required for cranial neural crest development in *Xenopus*. *Development* 129(2):421–432
  31. Perez-Alcala S, Nieto MA, Barbas JA (2004) LSox5 regulates RhoB expression in the neural tube and promotes generation of the neural crest. *Development* 131(18):4455–4465
  32. Barembaum M, Bronner ME (2013) Identification and dissection of a key enhancer mediating cranial neural crest specific expression of transcription factor, Ets-1. *Dev Biol* 382(2):567–575
  33. Nagai T, Aruga J, Takada S, Günther T, Spörle R, Schughart K, Mikoshiba K (1997) The expression of the mouse Zic1, Zic2, and Zic3 gene suggests an essential role for Zic genes in body pattern formation. *Dev Biol* 182(2):299–313
  34. Teslaa JJ, Keller AN, Nyholm MK, Grinblat Y (2013) Zebrafish Zic2a and Zic2b regulate neural crest and craniofacial development. *Dev Biol* 380(1):73–86
  35. Das A, Crump JG (2012) Bmps and id2a act upstream of Twist1 to restrict ectomesenchyme potential of the cranial neural crest. *PLoS Genet* 8:e1002710
  36. Machon O, Masek J, Machonova O, Krauss S, Kozmik Z (2015) Meis2 is essential for cranial and cardiac neural crest development. *BMC Dev Biol* 15:40
  37. Mitchell PJ, Timmons PM, Hébert JM, Rigby PW, Tjian R (1991) Transcription factor AP-2 is expressed in neural crest cell lineages during mouse embryogenesis. *Genes Dev* 5(1):105–119
  38. Shen H, Wilke T, Ashique AM, Narvey M, Zerucha T, Savino E, Williams T, Richman JM (1997) Chicken transcription factor AP-2: cloning, expression and its role in outgrowth of facial prominences and limb buds. *Dev Biol* 188(2):248–266
  39. Luo T, Lee YH, Saint-Jeannet JP, Sargent TD (2003) Induction of neural crest in *Xenopus* by transcription factor AP2alpha. *Proc Natl Acad Sci USA* 100(2):532–537
  40. Sauka-Spengler T, Meulemans D, Jones M, Bronner-Fraser M (2007) Ancient evolutionary origin of the neural crest gene regulatory network. *Dev Cell* 13(3):405–420
  41. Nikitina N, Sauka-Spengler T, Bronner-Fraser M (2008) Dissecting early regulatory relationships in the lamprey neural crest gene network. *Proc Natl Acad Sci USA* 105(51):20083–20088
  42. Khudyakov J, Bronner-Fraser M (2009) Comprehensive spatiotemporal analysis of early chick neural crest network genes. *Dev Dyn* 238(3):716–723
  43. de Crozé N, Maczkowiak F, Monsoro-Burq AH (2011) Reiterative AP2a activity controls sequential steps in the neural crest gene regulatory network. *Proc Natl Acad Sci USA* 108(1):155–160
  44. Wang WD, Melville DB, Montero-Balaguer M, Hatzopoulos AK, Knapik EW (2011) Tfap2a and Foxd3 regulate early steps in the development of the neural crest progenitor population. *Dev Biol* 360(1):173–185
  45. Powell DR, Hernandez-Lagunas L, LaMonica K, Artinger KB (2013) Prdm1a directly activates foxd3 and tfap2a

- during zebrafish neural crest specification. *Development* 140(16):3445–3455
46. Yang L, Zhang H, Hu G, Wang H, Abate-Shen C, Shen MM (1998) An early phase of embryonic *Dlx5* expression defines the rostral boundary of the neural plate. *J Neurosci* 18(20):8322–8330
  47. Luo T, Matsuo-Takasaki M, Lim JH, Sargent TD (2001) Differential regulation of *Dlx* gene expression by a BMP morphogenetic gradient. *Int J Dev Biol* 45(4):681–684
  48. Li B, Kuriyama S, Moreno M, Mayor R (2009) The posteriorizing gene *Gbx2* is a direct target of Wnt signalling and the earliest factor in neural crest induction. *Development* 136(19):3267–3278
  49. Hill RE, Jones PF, Rees AR, Sime CM, Justice MJ, Copeland NJ, Jenkins NA, Graham E, Davidson DR (1998) A new family of mouse homeo box-containing genes: molecular structure, chromosomal location, and developmental expression of *Hox-7.1*. *Genes Dev* 3(1):26–37
  50. Suzuki A, Ueno N, Hemmati-Brivanlou A (1997) *Xenopus msx1* mediates epidermal induction and neural inhibition by BMP4. *Development* 124(16):3037–3044
  51. Simões-Costa M, McKeown SJ, Tan-Cabugao J, Sauka-Spengler T, Bronner ME (2012) Dynamic and differential regulation of stem cell factor *FoxD3* in the neural crest is encrypted in the genome. *PLoS Genet* 8:e1003142
  52. Goulding MD, Chalepakis G, Deutsch U, Erselius JR, Gruss P (1991) *Pax-3*, a novel murine DNA binding protein expressed during early neurogenesis. *EMBO J* 10(5):1135–1147
  53. Bang AG, Papalopulu N, Goulding MD, Kintner C (1999) Expression of *Pax-3* in the lateral neural plate is dependent on a Wnt-mediated signal from posterior nonaxial mesoderm. *Dev Biol* 212(2):366–380
  54. Alkobtawi M, Ray H, Barriga EH, Moreno M, Kerney R, Monsoro-Burq AH, Saint-Jeannet JP, Mayor R (2018) Characterization of *Pax3* and *Sox10* transgenic *Xenopus laevis* embryos as tools to study neural crest development. *Dev Biol* 444(17):30693–30700
  55. Maczkowiak F, Matéos S, Wang E, Roche D, Harland R, Monsoro-Burq AH (2010) The *Pax3* and *Pax7* paralogs cooperate in neural and neural crest patterning using distinct molecular mechanisms, *Xenopus laevis* embryos. *Dev Biol* 340(2):381–396
  56. Nakata K, Nagai T, Aruga J, Mikoshiba K (1998) *Xenopus Zic* family and its role in neural crest development. *Mech Dev* 75(1–2):43–51
  57. Dottori M, Gross MK, Labosky P, Goulding M (2001) The winged helix transcription factor *Foxd3* suppresses interneuron differentiation and promotes neural crest cell fate. *Development* 128(21):4127–4138
  58. Kos R, Reedy MV, Johnson RL, Erickson CA (2001) The winged-helix transcription factor *FoxD3* is important for establishing the neural crest lineage and repressing melanogenesis in avian embryos. *Development* 128(8):1467–1479
  59. Wilson YM, Richards KL, Ford-Perriss ML, Panthier JJ, Murphy M (2004) Neural crest cell lineage segregation in the mouse neural tube. *Development* 131(24):6153–6162
  60. Liu L, Chong SW, Balasubramanian NV, Korzh V, Ge R (2002) Platelet-derived growth factor receptor alpha (*pdgfr- $\alpha$* ) gene in zebrafish embryonic development. *Mech Dev* 116:227–230
  61. Liu KJ, Harland RM (2003) Cloning and characterization of *Xenopus Id4* reveals differing roles for *Id* genes. *Dev Biol* 264(2):339–351
  62. Figueiredo AL, Maczkowiak F, Borday C, Pla P, Sittewelle M, Pegoraro C, Monsoro Burq AH (2017) PFKFB4 control of AKT signaling is essential for premigratory and migratory neural crest formation. *Development* 144(22):4183–4194
  63. Yang X, Li J, Zeng W, Li C, Mao B (2016) Elongator protein 3 (*Elp3*) stabilizes *Snail1* and regulates neural crest migration in *Xenopus*. *Sci Rep* 6:26238
  64. Sefton M, Sánchez S, Nieto MA (1998) Conserved and divergent roles for members of the Snail family of transcription factors in the chick and mouse embryo. *Development* 125(16):3111–3121
  65. del Barrio MG, Nieto MA (2002) Overexpression of Snail family members highlights their ability to promote chick neural crest formation. *Development* 129(7):1583–1593
  66. Aybar MJ, Nieto MA, Mayor R (2003) Snail precedes Slug in the genetic cascade required for the specification and migration of the *Xenopus* neural crest. *Development* 130(3):483–494
  67. Nieto MA, Sargent MG, Wilkinson DG, Cooke J (1994) Control of cell behavior during vertebrate development by *Slug*, a zinc finger gene. *Science* 264(5160):835–859
  68. Jiang R, Lan Y, Norton CR, Sundberg JP, Gridley T (1998) The *Slug* gene is not essential for mesoderm or neural crest development in mice. *Dev Biol* 198(2):277–285
  69. Tien CL, Jones A, Wang H, Gerigk M, Nozell S, Chang C (2015) *Snail2/Slug* cooperates with Polycomb repressive complex 2 (*PRC2*) to regulate neural crest development. *Development* 142(4):722–731
  70. Martin BL, Harland RM (2001) Hypaxial muscle migration during primary myogenesis in *Xenopus laevis*. *Dev Biol* 239(2):270–280
  71. Cheung M, Briscoe J (2003) Neural crest development is regulated by the transcription factor *Sox9*. *Development* 130(23):5681–5693
  72. Cheung M, Chaboissier MC, Mynett A, Hirst E, Schedl A, Briscoe J (2005) The transcriptional control of trunk neural crest induction, survival, and delamination. *Dev Cell* 8(2):179–192
  73. Honoré SM, Aybar MJ, Mayor R (2003) *Sox10* is required for the early development of the prospective neural crest in *Xenopus* embryos. *Dev Biol* 260(1):79–96
  74. McKeown SJ, Lee VM, Bronner-Fraser M, Newgreen DF, Farlie PG (2005) *Sox10* overexpression induces neural crest-like cells from all dorsoventral levels of the neural tube but inhibits differentiation. *Dev Dyn* 233(2):430–444
  75. Prasad MK, Reed X, Gorkin DU, Cronin JC, McAdow AR, Chain K, Hodonsky CJ, Jones EA, Svaren J, Antonellis A, Johnson SL, Loftus SK, Pavan WJ, McCallion AS (2011) *SOX10* directly modulates *ERBB3* transcription via an intronic neural crest enhancer. *BMC Dev Biol* 11:40
  76. Baggiolini A, Varum S, Mateos JM, Bettosini D, John N, Bonalli M, Ziegler U, Dimou L, Clevers H, Furrer R, Sommer L (2015) Premigratory and migratory neural crest cells are multipotent in vivo. *Cell Stem Cell* 16(3):314–322
  77. McKinney MC, McLennan R, Kulesa PM (2016) Angiopoietin 2 signaling plays a critical role in neural crest cell migration. *BMC Biol* 14(1):111
  78. Lee HO, Levorse JM, Shin MK (2003) The endothelin receptor-B is required for the migration of neural crest-derived melanocyte and enteric neuron precursors. *Dev Biol* 259(1):162–175
  79. Giovannone D, Ortega B, Reyes M, El-Ghali N, Rabadi M, Sao S, de Bellard ME (2015) Chicken trunk neural crest migration visualized with HNK1. *Acta Histochem* 117(3):255–266
  80. Zuhdi N, Ortega B, Giovannone D, Ra H, Reyes M, Asención V, McNicoll I, Ma L, de Bellard ME (2012) Slits affect the timely migration of neural crest cells via robo receptor. *Dev Dyn* 241(8):1274–1288
  81. Chiovaro F, Chiquet-Ehrismann R, Chiquet M (2015) Transcriptional regulation of tenascin genes. *Cell Adhes Migr* 9(1–2):34–47

82. Taneyhill AL, Coles EG, Bronner-Fraser M (2007) Snail2 directly represses cadherin6B during epithelial-to-mesenchymal transitions of the neural crest. *Development* 134(8):1480–1490
83. Groysman M, Shoval I, Kalcheim C (2008) A negative modulatory role for rho and rho-associated kinase signaling in delamination of neural crest cells. *Neural Dev* 3:27
84. Vega FM, Thomas M, Reymond N, Ridley AJ (2015) The Rho GTPase RhoB regulates cadherin expression and epithelial cell-cell interaction. *Cell Commun Signal* 13:6
85. Liu Q, Dalman MR, Sarmah S, Chen S, Chen Y, Hurlbut AK, Spencer MA, Pancoe L, Marrs JA (2011) Cell adhesion molecule cadherin-6 function in zebrafish cranial and lateral line ganglia development. *Dev Dyn* 240(7):1716–1726
86. Tomczuk M, Takahashi Y, Huang J, Murase S, Mistretta M, Klaffky E, Sutherland A, Bolling L, Coonrod S, Marcinkiewicz C, Sheppard D, Stepp MA, White JM (2003) Role of multiple beta1 integrins in cell adhesion to the disintegrin domains of ADAMs 2 and 3. *Exp Cell Res* 290(1):68–81
87. Desanlis I, Felstead HL, Edwards DR, Wheeler GN (2018) ADAMTS9, a member of the ADAMTS family, in *Xenopus* development. *Gene Expr Patterns* 29:72–81
88. Porter S, Clark IM, Kevorkian L, Edwards DR (2005) The ADAMTS metalloproteinases. *Biochem J* 386(1):15–27
89. Hubmacher D, Apte SS (2015) ADAMTS proteins as modulators of microfibril formation and function. *Matrix Biol* 47(2015):34–43
90. Chen WV, Maniatis T (2013) Clustered protocadherins. *Development* 140(16):3297–3302
91. Okawa T, Kamiya H, Himeno T, Kato J, Seino Y, Fujiya A, Kondo M, Tsunekawa S, Naruse K, Hamada Y, Ozaki N, Cheng Z, Kito T, Suzuki H, Ito S, Oiso Y, Nakamura J, Isobe K (2013) Transplantation of neural crest-like cells derived from induced pluripotent stem cells improves diabetic polyneuropathy in mice. *Cell Transplant* 22(10):1767–1783
92. Seki D, Takeshita N, Oyanagi T, Sasaki S, Takano I, Hasegawa M, Takano-Yamamoto T (2015) Differentiation of odontoblast-like cells from mouse induced pluripotent stem cells by Pax9 and Bmp4 transfection stem cells. *Transl Med* 4(9):993–997
93. Mizuseki K, Sakamoto T, Watanabe K, Muguruma K, Ikeya M, Nishiyama A, Arakawa A, Suemori H, Nakatsuji N, Kawasaki H, Murakami F, Sasai Y (2003) Generation of neural crest-derived peripheral neurons and floor plate cells from mouse and primate embryonic stem cells. *Proc Natl Acad Sci USA* 100(10):5828–5833
94. Motohashi T, Aoki H, Chiba K, Yoshimura N, Kunisada T (2007) Multipotent cell fate of neural crest-like cells derived from embryonic stem cells. *Stem Cells* 25(2):402–412
95. Kawaguchi J, Nichols J, Gierl MS, Faial T, Smith A (2010) Isolation and propagation of enteric neural crest progenitor cells from mouse embryonic stem cells and embryos. *Development* 137(5):693–704
96. Aihara Y, Hayashi Y, Hirata M, Arika N, Shibata S, Nagoshi N, Nakanishi M, Ohnuma K, Warashina M, Michiue T, Uchiyama H, Okano H, Asashima M, Furue MK (2010) Induction of neural crest cells from mouse embryonic stem cells in a serum-free monolayer culture. *Int J Dev Biol* 54(8–9):1287–1294
97. Minamino Y, Ohnishi Y, Kakudo K, Nozaki M (2015) Isolation and propagation of neural crest stem cells from mouse embryonic stem cells via cranial neurospheres. *Stem Cells Dev* 24(2):172–181
98. Lee G, Chambers SM, Tomishima MJ, Studer L (2010) Derivation of neural crest cells from human pluripotent stem cells. *Nat Protoc* 5(4):688–701
99. Wang A, Tang Z, Li X, Jiang Y, Tsou DA, Li S (2012) Derivation of smooth muscle cells with neural crest origin from human induced pluripotent stem cells. *Cells Tissues Organs* 195(1–2):5–14
100. Kreitzer FR, Salomonis N, Sheehan A, Huang M, Park JS, Spindler MJ, Lizarraga P, Weiss WA, So PL, Conklin BR (2013) A robust method to derive functional neural crest cells from human pluripotent stem cells. *Am J Stem Cells* 2(2):119–131
101. Tomokiyo A, Hynes K, Ng J, Menicanin D, Camp E, Arthur A, Gronthos S, Mark Bartold P (2017) Generation of neural crest-like cells from human periodontal ligament cell-derived induced pluripotent stem cells. *J Cell Physiol* 232(2):402–416
102. Michael D, Wagoner MD, Bohrer LR, Aldrich BT, Greiner MA, Mullins RF, Worthington KS, Tucker BA, Wiley LA (2018) Feeder-free differentiation of cells exhibiting characteristics of corneal endothelium from human induced pluripotent stem cells. *Biol Open* 7(5):bio032102
103. Pomp O, Brokhman I, Ben-Dor I, Reubinoff B, Goldstein RS (2005) Generation of peripheral sensory and sympathetic neurons and neural crest cells from human embryonic stem cells. *Stem cells* 23(7):923–930
104. Lee G, Kim H, Elkabetz Y, Al Shamy G, Panagiotakos G, Barberi T, Tabar V, Studer L (2007) Isolation and directed differentiation of neural crest stem cells derived from human embryonic stem cells. *Nat Biotechnol* 25(12):1468–1475
105. Liu Q, Spusta SC, Mi R, Lassiter RN, Stark MR, Höke A, Rao MS, Zeng X (2012) Human neural crest stem cells derived from human ESCs and induced pluripotent stem cells: induction, maintenance, and differentiation into functional schwann cells. *Stem Cells Transl Med* 1(4):266–278
106. Noisa P, Lund C, Kanduri K, Lund R, Lähdesmäki H, Lahesmaa R, Lundin K, Chokeychuwattanalert H, Otonkoski T, Tuuri T, Raivio T (2014) Notch signaling regulates the differentiation of neural crest from human pluripotent stem cells. *J Cell Sci* 127:2083–2094
107. Karbalaie K, Tanhaei S, Rabiei F, Kiani-Esfahani A, Masoudi NS, Nasr-Esfahani MH, Baharvand H (2015) Stem cells from human exfoliated deciduous tooth exhibit stromal-derived inducing activity and lead to generation of neural crest cells from human embryonic stem cells. *Cell J* 17(1):37–48
108. Avery J, Dalton S (2016) Methods for derivation of multipotent neural crest cells derived from human pluripotent stem cells. *Methods Mol Biol* 1341:197–208
109. Zhang JT, Weng ZH, Tsang KS, Tsang LL, Chan HC, Jiang XH (2016) MycN is critical for the maintenance of human embryonic stem cell-derived neural crest stem cells. *PLoS One* 11:e0148062
110. Lovatt M, Yam GH, Peh GS, Colman A, Dunn NR, Mehta JS (2018) Directed differentiation of periocular mesenchyme from human embryonic stem cells. *Differentiation* 99:62–69
111. Dennis AR, McLennan R, Jessica MT, Craig LS, Jeffrey SH, Kulesa PM (2014) The neural crest cell cycle is related to phases of migration in the head. *Development* 141(5):1095–1103
112. Krishnakumar R, Chen AF, Pantovich MG, Danial M, Parchem RJ, Labosky PA, Belloch R (2016) FOXD3 regulates pluripotent stem cell potential by simultaneously initiating and repressing enhancer activity. *Cell Stem Cell* 18(1):104–117

**Publisher's Note** Springer Nature remains neutral with regard to jurisdictional claims in published maps and institutional affiliations.